ACI STRUCTURAL JOURNAL TECHNICAL PAPER

Title no. 100-S6

Towards Modeling of Reinforced Concrete Members with Externally Bonded Fiber-Reinforced Polymer Composites

by Rita S. Y. Wong and Frank J. Vecchio

Fiber-reinforced polymer (FRP) composites have been increasingly studied for their application in the flexural or shear strengthening of reinforced concrete (RC) members. Although substantial increases in strength have been achieved, reductions in ductility have also been reported as a result of debonding failures near the concrete-FRP interface. The debonding phenomenon is the subject of the experimental program described herein, which involved the strengthening of shear-critical beams using carbon FRP (CFRP) strips. It has been determined that the bond-slip behavior at the bond interface must be considered in the numerical modeling of externally reinforced members. Essential to analyses using a finite element program are the formulations of bond elements and their constitutive relations. The implementation of link and contact elements, along with linear elastic and elastic-plastic bond laws, is shown to produce accurate predictions of member response.

Keywords: bond; fiber-reinforced polymer; reinforced concrete; slip.

INTRODUCTION

Fiber-reinforced polymer (FRP) laminates have gained popularity as external reinforcement for the strengthening or rehabilitation of reinforced concrete (RC) structures. Numerous experimental studies have shown that externally bonded FRPs can significantly increase a member's stiffness and load-carrying capacity. On the other hand, there have also been reports of reduction in ductility associated with brittle behavior due to mechanisms such as bond failure, as noted by Arduini and Nanni[1] and Ross et al.[2] Such premature failure leads to inefficient usage of the FRP material and prevents the strengthened members from reaching their full capacities.

Although the experimental database for RC members strengthened in flexure with FRP composites is extensive, further investigations are imperative in the domain of shear strengthening. The failure modes of flexural-strengthened members have been analyzed thoroughly by numerous researchers, but the complexities involved with shear behavior require more attention. Therefore, an experimental program was undertaken to study the debonding phenomenon in RC beams strengthened in shear with carbon FRP (CFRP) composites. Three full-size beams shear reinforced with CFRP strips were tested; their performance and failure modes are discussed in this paper.

In the realm of numerical analysis work, limited literature is available regarding RC members shear strengthened with FRP composites. Among the studies that have been carried out using the finite element method, few have included the effects of FRP debonding. For example, Vecchio and Bucci[3] reported that results from a nonlinear finite element program showed reasonably good agreement with experimental data in terms of the enhanced stiffness of the strengthened flexural members. It was noted, however, that the numerical program tended to overestimate the failure loads of the members because debonding failure was not considered. Therefore, more attention is required in numerical modeling to account for the possibility of debonding failures.

To accurately predict the ultimate capacity and failure mode of RC members reinforced with FRP laminates, it is necessary to model the bond at the concrete-FRP interface that provides load transfer between the two components. Because debonding failure is governed by the local bond stress-slip relationship at the interface, one must account for the relative displacement between FRP and concrete. How this can be accomplished through the incorporation of interface elements, such as link or contact elements, in the finite element modeling will be investigated in this paper. Corroboration with four sets of specimens (including the shear-strengthened beams tested in the experimental program described herein) will be used to verify the finite element analyses.

RESEARCH SIGNIFICANCE

Within the past 10 years, much research has been conducted in the area of repair and application techniques of FRP materials for RC structures. In addition, work has progressed in the development of design procedures and code specifications. More studies in numerical modeling are required, however, particularly with regards to the debonding phenomenon of FRP composites and in shear applications. This paper will address these deficiencies.

EXPERIMENTAL PROGRAM

Test specimens

The design of these three large-scale beams was based on the series of OA beams tested by Bresler and Scordelis.[4] The RWOA beams were modeled after the OA beams, which did not contain internal shear reinforcement but were subsequently shear strengthened by bonding CFRP strips onto the side surfaces of the beams. (Three control specimens without the CFRP reinforcement were also tested.) The cross-sectional dimensions of all three beams measured 305 x 560 mm (Fig. 1), while the details of the specimens are presented in Table 1. An elevation view of the beams, showing the bonding configuration of the CFRP strips, is given in Fig. 2. At the ends of the beams, 25 mm-thick plates were welded to the flexural steel to enhance anchorage of the reinforcing bars as flexural failure might ensue due to the presence of the CFRP strips.

The CFRP fabric used was composed of graphite fibers oriented in the longitudinal direction and Kevlar 49 weft in

ACI Structural Journal, V. 100, No. 1, January-February 2003.
MS No. 01-348 received October 19, 2001, and reviewed under Institute publication policies. Pertinent discussion will be published in the November-December 2003 *ACI Structural Journal* if received by July 1, 2003.

Rita S. Y. Wong *is a structural designer, Yolles Partnership Inc., Toronto. She received her BSc from the University of Manitoba and her MASc in structural engineering from the University of Toronto.*

ACI member **Frank J. Vecchio** *is Professor and Associate Chair in the Department of Civil Engineering, University of Toronto, Toronto, Ontario, Canada. He is a member of Joint ACI-ASCE Committees 441, Reinforced Concrete Columns, and 447, Finite Element Analysis of Reinforced Concrete Structures. His research interests include nonlinear analysis and design of concrete structures, constitutive modeling, assessment, and repair and rehabilitation of structures.*

the perpendicular direction. This fabric, with a measured average thickness of 0.84 mm, was tested in accordance with ASTM D 3039/D 3039M.[5] A tensile strength of 1090 MPa and an ultimate strain of 0.011 were recorded. CFRP strips of 200 mm width, spaced at 300 mm on center, were bonded only onto the sides of the beams (not wrapped around the top or bottom surfaces) to promote debonding. For the bonding procedure, a two-part epoxy adhesive, consisting of Components A and B, was applied. The tensile strength and elastic modulus of the epoxy were specified by the manufacturer to be 72 and 3 MPa, respectively. The mixing ratio was 100 parts of A to 42 parts of B (by volume), and 1 L of epoxy was mixed for each square meter of area to be covered. A mechanical mixer was used to mix the two components together for 5 min at a speed of 400 to 600 rpm until uniform.

After the beams were cured at room temperature for at least 28 days, the side surfaces were sprayed with a water jet to remove all loose particles. Bonding of the CFRP strips took place once the beams were air dried. One coat of epoxy was applied, using paint rollers, to the concrete surface to allow for some penetration into the concrete cover. Both sides of the CFRP strips were covered with epoxy to ensure saturation of the fibers. The beam and CFRP strips were left exposed to air for 2 h until the epoxy thickened and became sticky. Epoxy was reapplied to parts of the concrete where the first coat had been absorbed from the surface. Then the strips of CFRP fabric were attached onto the beam with care taken to straighten the fibers, as the fabric tended to fold under the weight of the epoxy. The thickness of the epoxy was not measured, but any excess was squeezed out when the CFRP strips were smoothed with a wallpaper smoother. This was done to remove air bubbles and to ensure complete epoxy coverage. A final coat of epoxy (over the CFRP strips) was omitted as the weight of the added epoxy caused the strips to slide down the sides of the beam.

Table 1—Details of test specimens

Specimen reference	Span, m	Concrete compressive strength, MPa	Steel reinforcement			
			25M*		30M†	
			Yield strength, MPa	Ultimate strength, MPa	Yield strength, MPa	Ultimate strength, MPa
RWOA-1	3.66	22.6	445	680	436	700
RWOA-2	4.57	25.9	440	615	436	700
RWOA-3	6.40	43.5	445	680	436	700

*A_s = 500 mm^2
†A_s = 700 mm^2

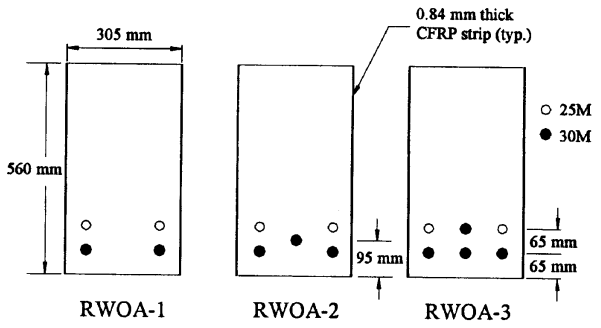

Fig. 1—Cross section details of RWOA beams.

Test procedure

The beams were tested under monotonic three-point loading after the epoxy had cured at room temperature for at least 10 days. A thin layer of gypsum plaster sitting on steel plates was used to disperse loads and reactions from pin and roller supports. All specimens were tested using a servohydraulic MTS testing machine. A load cell connected to the data acquisition system measured the applied load. Midspan deflection was measured using two linear variable differential transformers (LVDTs)—one at the north face and the other at the south face. Two LVDTs were also set up at opposite faces of the two supports to detect any support settlements. Loading proceeded in increments of 20 kN until yielding of the longitudinal reinforcement, at which time loading was applied in terms of midspan displacement. Surface strains at the level of the longitudinal reinforcement were recorded through the horizontal displacements of 12 Zurich targets bonded on each side of the beam. All measured displacements were directly recorded by the data acquisition system. Cracks noted

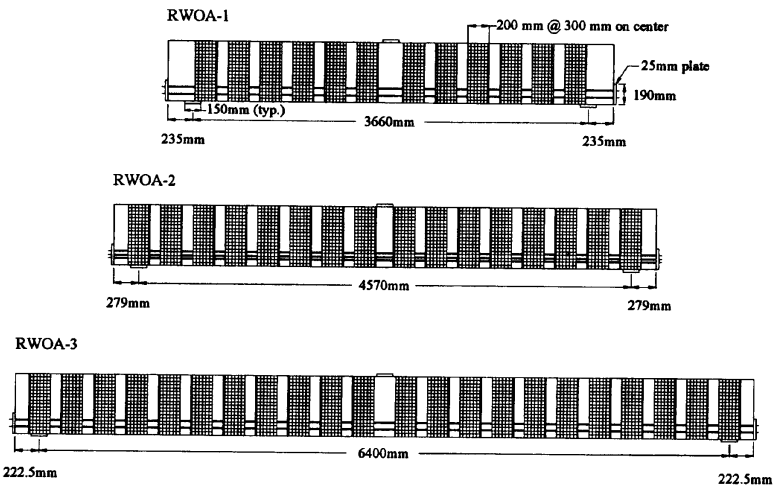

Fig. 2—Elevation views of RWOA beams.

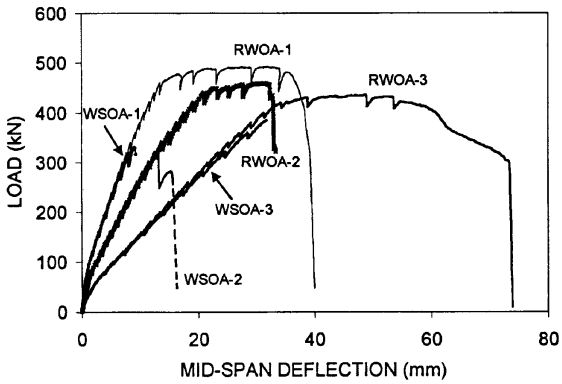

Fig. 3—Load-deflection curves for WSOA and RWOA beams.

on the side concrete surfaces were marked and their widths were measured at every load stage.

Test observations and results

The appearance of flexural cracks was first noted on the bottom surface at approximately 80 kN for all three beams. The presence of the CFRP strips and the darkened concrete side surface (due to the epoxy coating), however, may have obscured cracks that had formed earlier. Flexural and shear cracks formed and widened as loading proceeded. Yielding of the flexural steel occurred in all three specimens, leading to the widening of flexural cracks at midspan. The beams experienced shear-flexural failure while exhibiting ductile behavior, with concrete crushing near the loading point, as major shear cracks formed. The maximum widths ranged from 1.6 to 3.5 mm for flexural cracks and from 0.15 to 0.20 mm for shear cracks. Some cracks formed at the vertical edge of a few CFRP strips, and as these cracks widened, the CFRP strips appeared to be on the verge of peeling. The maximum loads sustained by the beams were as follows: 493 kN at a midspan deflection of 35 mm for RWOA-1, 457 kN at 32 mm deflection for RWOA-2, and 436 kN at 50 mm deflection for RWOA-3. The load-deflection curves for the beams are presented in Fig. 3, and are compared against the responses of control specimens (WSOA). The control beams were identical to the RWOA beams but without the CFRP strips.

The failure modes of the three RWOA beams were similar. Although premature debonding of the CFRP strips did not occur, portions of the strips above the shear crack did peel away from the beams at ultimate. A thin layer of concrete was visible on the back of the debonded strips. Once the CFRP strips had peeled away from the beam, the crushed concrete was exposed, the confinement effect was lost, and pieces of concrete spalled off. The strips that crossed the lower half of the shear cracks tore off with the concrete cover, causing the side cover to split out from the beam. This behavior was similarly observed on both the north and south sides of the beam. At ultimate, after the stiff side surfaces were pushed outwards, the central section of the beam, now unreinforced in shear, punched through. The outward push of the concrete cover also led to the partial splitting of some CFRP strips. Figure 4 shows the typical failure modes observed, while full details of the experimental results are given by Wong.[6]

Discussion of test results

While the WSOA control beams failed suddenly in brittle shear, the RWOA series, shear reinforced with CFRP strips, exhibited ductile behavior and a shear-flexural failure. The

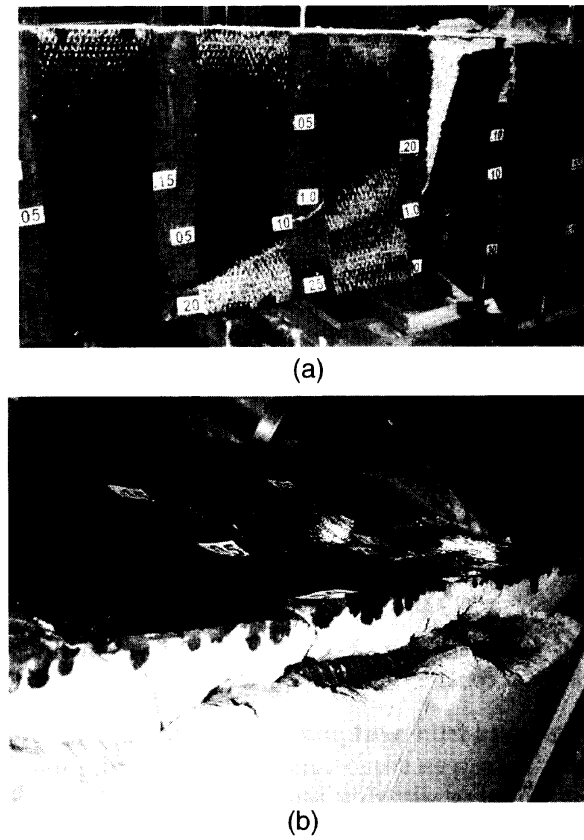

Fig. 4—Beam RWOA-2 at failure: (a) side view; and (b) bottom view.

vertically oriented CFRP strips prevented the brittle shear failure of the beams by acting in the same manner as stirrups. The strips exerted a closing effect on the shear cracks, limited their propagation, and increased the concrete's shear resistance by permitting more aggregate interlock to occur. This allowed the beam to sustain higher loads until the longitudinal reinforcement yielded in tension, achieving loads up to 50% higher than the control specimens. It also resulted in more ductile behavior, with midspan deflections up to 350% greater than the WSOA beams. However, the shear contribution by the CFRP strips decreased from 82 kN to 70 kN to 26 kN for beams RWOA-1 to RWOA-3. The degree of strength increase provided by the CFRP was limited by the yield strength of the flexural steel and the compressive capacity of the concrete.

At ultimate, crushing of the concrete and displacements near the shear crack caused the peeling of the CFRP strips above the shear crack. Below the shear crack, the high normal peeling forces at the end of the strips tore the stiffened concrete side cover away from the beam. Because the CFRP strips were bonded only to the side surfaces, the central section of the beam was unconfined after the outwards splitting of the side cover, causing it to punch out in a downward direction as a result of shear forces. No premature debonding of the CFRP strips was noted, which implies that the surface preparation of the beams was adequate and that the bond strength of the epoxy used was sufficiently high. It was observed that a thin layer of concrete remained attached to the CFRP strips after separation. This indicates that the lower shear strength of concrete had led to the debonding, rather than shear slippage within the epoxy layer or at the FRP-adhesive interface. This is consistent with the fact that the shear strength of epoxy is much higher than that of concrete.

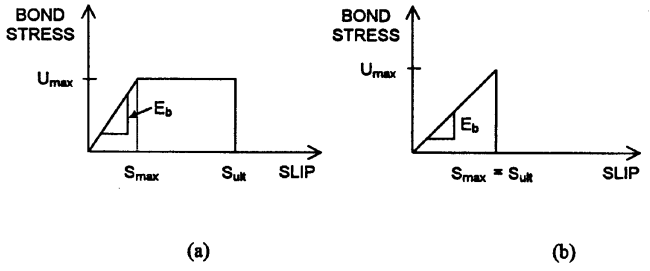

Fig. 5—Constitutive relationship for bond interface: (a) elastic-plastic; and (b) linear elastic.

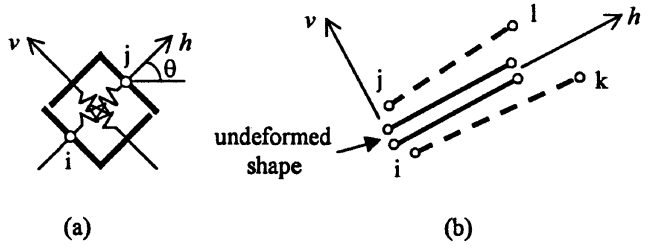

Fig. 6—Representation of: (a) link element; and (b) one-dimensional contact element.

Conclusions from test program

The results suggest that for aging beams in which the stirrups have corroded or where the shear reinforcement ratio does not satisfy updated standards, CFRP laminates may present a viable and convenient method for upgrading shear capacity. The CFRP composites can also be used to avert brittle shear failures, promoting more ductile flexural behavior with enhanced deflection capacity prior to failure. Peeling of the CFRP strips and separation of concrete side cover, however, can lead to punching failure of the beams. Therefore, for practical purposes, CFRP composites should be applied in a U-shaped configuration, and top edges of the CFRP strips should be anchored to the beam to prevent debonding failures. Further research is required.

FINITE ELEMENT ANALYSIS

A two-dimensional nonlinear finite element program was used for the numerical analyses. The program is based on the Modified Compression Field Theory by Vecchio and Collins.[7] It is based on a smeared, rotating crack model for RC, in which cracked concrete is represented as an orthotropic material with a unique constitutive relation. Appropriate models are used to represent second-order mechanisms in concrete behavior, including compression softening, tension stiffening and softening, and slip on the shear crack surface. Steel reinforcement is assumed to behave in an elastic-plastic manner with strain hardening effects, while FRP reinforcement is assumed to be linear elastic with brittle fracture in tension. The details of the constitutive models and their implementation into the finite element program have been previously described by Vecchio.[8,9]

Analyses of RC members bonded with FRP were previously conducted by Bucci (Vecchio and Bucci[3]) using a two-dimensional nonlinear finite element program. In his work, laminates bonded on concrete side surfaces were smeared into rectangular elements, which were then superimposed directly onto concrete elements. This implied perfect bond conditions between concrete and FRP, and led to overestimations of member stiffness and capacity. Thus, in the current research, slippage at the bond interface was taken into account to improve the accuracy of the simulations.

For the bond interface, various bond stress-slip relationships between concrete and FRP have been proposed. Among these are the linear elastic model used by Aprile, Spacone, and Limkatanyu[10] and the elastic-plastic models presented by Homam et al.[11] and Sato.[12] The parameters in these models include the maximum shear stress that can be sustained by the bond interface U_{max}, the slip at the first occurrence of maximum bond stress S_{max}, and the ultimate slip when the bond fails S_{ult}. The slope of the linear relationship is termed the slip modulus E_b and is based on the shear stiffness of the epoxy G_a used, as defined by Eq. (1)

$$E_b = \frac{G_a}{t_a} \quad \text{where} \quad G_a = \frac{E_a}{2(1+\nu_a)} \tag{1}$$

The variables E_a, t_a, and ν_a denote the Young's modulus, thickness, and Poisson's ratio of the adhesive layer, respectively. The values defining the bond stress-slip relationship (as determined from Homam's tests), in the order U_{max}, S_{max}, and S_{ult}, are: 3.5 MPa, 0.01 mm, and 0.50 mm for CFRP; and 2.5 MPa, 0.01 mm, and 0.67 mm for glass FRP (GFRP). A general shape of the elastic-plastic relationship, as seen in Fig. 5(a), has been adopted in the current research. A linear elastic relationship, shown in Fig. 5(b), can be specified by setting S_{max} equal to S_{ult}.

Bond elements

To model the debonding phenomenon accurately, interface or bond elements must be incorporated. Two appropriate bond element types are the link element and the one-dimensional contact element. To represent the bonding of FRP plates or sheets, the relevant concrete elements must be double noded. One set of nodes is used for the concrete elements, while the second set is used for the FRP (represented as truss elements). The nodes of these two adherents are connected by bond elements that allow relative displacement, or slip, to take place between concrete and FRP. The difference in displacement between the concrete node and the FRP node determines the nodal slip of the bond element. The bond stress is then calculated using the specified constitutive relationship. Finally, the force transferred by the bond element is found by multiplying the bond stress and the bonded surface area represented by the element.

The link element was developed by Ngo and Scordelis[13] in their analysis of bond-slip between steel reinforcing bars and concrete in RC beams. The link element has no physical dimensions, so the two nodes (i and j) that it connects have the same coordinates. A representation of the link element, shown in Fig. 6(a), consists of two linear springs parallel to a set of orthogonal axes h and v. The link element can be oriented at any arbitrary angle θ with the horizontal axis of the RC member. Each spring can translate in either the h or v direction, and the displacement in each direction is independent of the other. The springs represent the shear and normal stiffness of the adhesive connection, while transmitting shear and normal forces between the nodes. Because most debonding failures with thinner FRP plates or sheets are due to shear at the interface, a high stiffness value is assigned to the spring in the normal (v) direction. This essentially limits the link element to having two degrees of freedom along the direction of the FRP truss element.

The one-dimensional contact element, developed by Hoshino and Schafer (Keuser and Mehlhorn[14]), provides a continuous connection between two adjoining elements. It is an isoparametric element that, in its undeformed state, has no dimensions in the transverse direction. The simplest form has two double nodes and is based on a linear displacement function. In each pair of double nodes, one node is connected to a concrete element while the other node is connected to the FRP element. In the unloaded stage, the coordinates of the nodes at each end of the contact element are identical. Once loading begins, the nodes behave independently, resulting in relative displacements between the two connected points, as illustrated in Fig. 6(b). Similar to the link element, a large stiffness value is chosen for the normal direction. Thus, the contact element has four degrees of freedom, each along the direction of the FRP truss element.

CORROBORATION WITH TEST SPECIMENS

The response of four sets of experimental specimens was investigated with a two-dimensional nonlinear finite element program, using link or contact elements to model the concrete-FRP interface. (It was found that link and contact elements produced similar results; only the results for contact elements are presented herein.) These specimens involve slabs or beams that have been strengthened for flexure or shear with FRP laminates.

Žarnić specimens

The first set of flexural specimens modeled were the slab strips and beams tested at the University of Ljubljana, Slovenia, by Žarnić et al.[15] The slab strip specimens were 800 mm in width, 120 mm in depth, and 3250 mm in length. The beams were of the same length but with cross sections 200 mm wide x 300 mm deep; full details are provided by Žarnić et al. For each type of flexural member, one specimen was kept as the control while three were strengthened with CFRP plates. The CFRP plates used were 50 mm wide and 1.2 mm thick, and the epoxy layer was 2 mm thick. External bonding was undertaken prior to the application of four-point loading on the beams.

In the experiment, the slab strip control specimen failed at a total load of 36.5 kN; the CFRP-repaired slabs showed increased strength of 63 kN. For the control beam, the ultimate load was 86.5 kN, and the bonding of the CFRP plate raised the failure load to 116.8 kN. With both types of specimens, sudden failures occurred, caused by delamination of the plates below the concentrated load in the region of extensive flexural deformation and cracking. The debonding initiated in the middle third of the beams and propagated to the free ends by peeling off a thin layer of concrete.

Due to the symmetrical nature of the Žarnić specimens, only 1/2 of the beam span was modeled. To match the experimental conditions, displacement-controlled loading was applied. For the bond elements, the maximum shear strength was specified to be 3.0 MPa, which corresponded to the modulus of rupture of concrete for these specimens ($f_r = 0.6 \times [f_c']^{0.5}$), where f_c' is the 28-day compressive strength of concrete). This value was chosen because the failure mode of the specimens was dominated by peeling of the FRP and shearing along the concrete surface. The maximum slip value was calculated using E_b = 2370 MPa/mm.

The load-deflection curves from the numerical analyses for the slab strip are shown in Fig. 7(a). With bond-slip considered using the linear elastic model (FE-LE), the calculated

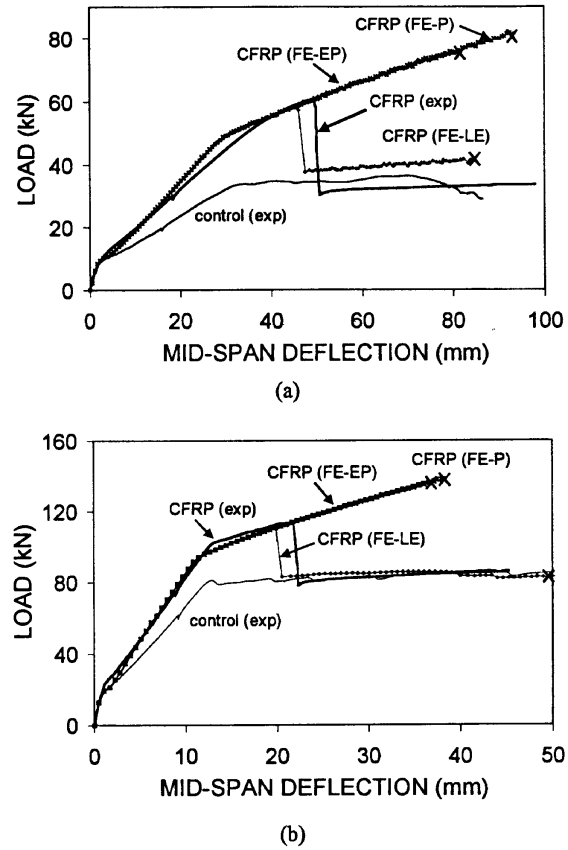

Fig. 7—Load-deflection curves for Žarnić specimens: (a) slab strips; and (b) beams.

failure load of 58 kN and the corresponding midspan deflection were within 5% of the average experimental values. The mode of failure of the strengthened specimen was by debonding of the CFRP plates, initiated under the loading point, as reported by Žarnić et al. With the elastic-plastic bond law (FE-EP), the peak load and deflection were overestimated by 22 and 73%, respectively. Note that assuming perfect bond conditions (FE-P) resulted in a predicted failure load 33% higher than the actual force sustained, at a midspan deflection that was twice as large as the experimental value.

For the beam specimens, the properties of the bond elements were the same as those used for the slab strip analyses because the same types of FRP and epoxy were used for both sets of specimens. As can be observed from Fig. 7(b), accounting for bond slip with the linear elastic bond law produced a reasonably accurate predicted response (FE-LE), with a failure load of 111 kN—5% lower than the test value. On the other hand, the elastic-plastic relationship (FE-EP) gave values of ultimate load and deflection that were 17 and 59% higher than the test data. The perfect bond condition (FE-P) overestimated the failure load by 19%, with a corresponding midspan deflection 66% larger than the experimental value.

El-Refaie specimens

The second set of specimens analyzed was a series of five RC continuous beams tested by El-Refaie, Ashour, and Garrity[16] at the University of Bradford, UK. Of the five two-span beams, one was tested as a control specimen (Beam CB1), while the remaining four (Beams CB2 to CB5) were strengthened with CFRP laminates. The dimensions of the beams were identical, each being 8500 mm long x 150 mm

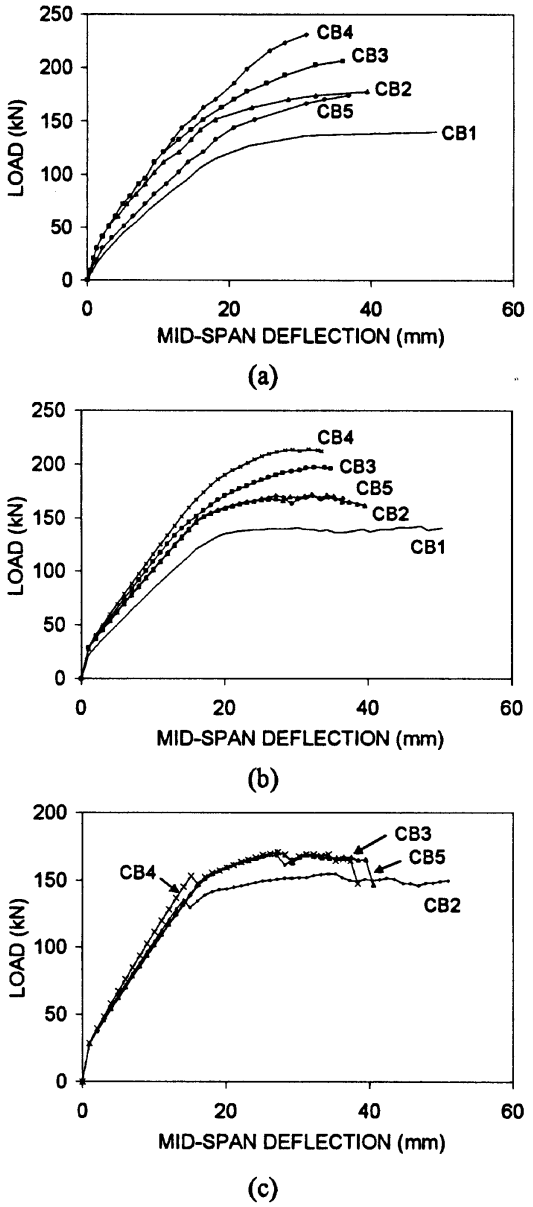

Fig. 8—Load-deflection curves for El-Refaie specimens: (a) experimental; (b) analytical using elastic-plastic bond law; and (c) analytical using linear elastic bond law.

wide x 250 mm deep. Beams CB2 to CB4 were strengthened with CFRP plates 100 mm wide x 1.2 mm thick. The locations of the plates were as follows: top face for CB2, bottom face for CB3, and both top and bottom faces for CB4. For Beam CB5, CFRP sheets of 110 mm width and a total thickness of 0.7 mm were bonded to the top face. Details of the beam geometry and materials used are given by El-Refaie, Ashour, and Garrity.[16]

Each beam, with a span length of 3830 mm, was subjected to center-point loading. The load-deflection curves for all five beams are plotted in Fig. 8(a). Ultimate loads for the strengthened CB beams were 17 to 54% higher than the control beam, and these beams attained an increase of approximately 50% in their moment capacities. While the control beam experienced a ductile failure, the strengthened beams all failed by peeling of the concrete cover adjacent to the CFRP laminates. Failure was brittle and occurred suddenly.

The symmetry and identical geometry of the beams allowed one mesh to be defined for one span of all five beams. Because peeling of the concrete cover arises from shearing along a horizontal plane, the modulus of rupture was used as the tensile strength for the concrete cover. (This value is higher than $f'_t = 0.33 \times [f'_c]^{0.5}$), which is usually used as the tensile strength for diagonal tension due to shear.) Also, the modulus of rupture for the concrete was chosen as the maximum shear strength of the bond elements. The lower modulus of rupture led to the failure of the concrete cover, while the higher tensile strength of the epoxy kept the CFRP composites intact with the concrete. To determine S_{max} for the bond elements, the slip modulus was calculated for each beam using Eq. (1) (values of $\nu_a = 0.35$ and $t_a = 2$ mm were assumed). For the trial employing the elastic-plastic constitutive relationship, a value of 0.10 mm was used for S_{ult}. Details of the loading method were not reported in the original paper; hence, displacement-controlled loading was assumed in the analyses.

The analytical load-displacement curves show that the stiffness of the response, the ultimate loads, and the midspan deflections at maximum load were in good agreement with the experimental data. Overall, the analyses with the elastic-plastic bond model, depicted in Fig. 8(b), conservatively underestimated the ultimate loads by up to 7%. The linear elastic bond law predicted failure loads for Beams CB3 and CB4 that were 20% lower than the actual values, however, as seen in Fig. 8(c). The CFRP plates on these beams, being bonded on the soffit, experienced slips beyond the specified S_{ult} value, and failed prematurely in the analyses. Beam CB1 experienced a flexural failure, as was observed in the experiment. For Beams CB2 to CB5, which were strengthened with CFRP laminates, the dominant failure mode in the analyses was by shearing of the concrete cover adjacent to the CFRP. This led to the delamination of the composites as the bond interface failed in shear. The predicted failure mode was in good agreement with the experimental results.

De Rose specimens

The third set of specimens modeled numerically was the De Rose[17] series of slabs and beams tested at the University of Toronto. These specimens were constructed to simulate a wall panel (hereafter referred to as the slab) and a beam in a reinforced concrete parking structure in need of repair.

Three slab specimens were fabricated and tested: one as a control specimen, one repaired with CFRP, and another repaired with GFRP. Details of the specimens are provided by De Rose and Sheikh.[17] The control specimen was tested as-built to failure, while the other two specimens were preloaded and then repaired with the composite materials before loading to failure.

The control specimen failed in flexure at a load of 193 kN. The specimen that was to be repaired with CFRP was loaded to 135 kN, at which time three strips of CFRP fabric, each 600 mm in width and approximately 1 mm in thickness, were applied to the soffit of the slab. Loading on the slab continued until the specimen failed in shear at a total load of 478 kN, accompanied by large inclined cracks and delamination of CFRP. The third specimen was repaired and tested in a similar manner, except that GFRP fabric was used. This slab also failed in shear, but at a lower load of 422 kN. The failure of the repaired slabs was governed by their shear capacities, while no occurrence of premature FRP bond failure was noted.

The symmetrical geometric and loading conditions of the De Rose slab permitted modeling of only 1/2 of the specimen. The properties of the epoxy were not measured in the

experiment, so the values chosen for the elastic-plastic bond stress-slip relationship were based on bond experiments performed by Homam, who used the same type of epoxy and FRP fabric as De Rose. To match the experimental conditions, displacement-controlled monotonic loading was applied. Because the slabs were preloaded to an advanced load stage prior to the application of the FRP fabric, a two-stage analysis was required. In the first part of the analysis, only the elements in the control slab were engaged. Analysis was carried out to the load stage corresponding to the load at which the slab was repaired. Then the elements representing the repair materials were activated and the analysis was continued.

The load-deflection curves for the CFRP-repaired slab are given in Fig. 9(a) along with the experimental results. The ultimate load calculated by the elastic-plastic analysis (FE-EP) was 436 kN—9% lower than the actual failure load. Although the stiffness of the member immediately after repair was underestimated by the analysis, the postcracking stiffness and maximum load achieved were in close agreement with the experimental results. On the other hand, the perfect bond conditions (indicated by FE-P, a trial conducted by Bucci) overestimated the member's stiffness and failure load, while a premature failure was predicted by the linear elastic bond law (FE-LE). As observed in the experiment, the numerical modeling predicted a shear failure for the CFRP-repaired slab. The response of the GFRP-repaired slab and the curve obtained from the test are plotted in Fig. 9(b). Accounting for bond slip using FE-EP, the slab was predicted to fail at 394 kN, which was 7% lower than the experimental ultimate load. Similar to the CFRP-repaired slab, the perfect bond assumption (FE-P) led to over-predictions of stiffness and capacity.

Two haunched deep beams were also tested by De Rose: one was used as a control specimen while the second beam was shear strengthened with CFRP fabric. The specimen details are given by De Rose.[17] The control specimen failed in shear at a load of approximately 1700 kN. The beam to be repaired with CFRP was preloaded to 1180 kN, and this load was maintained while the CFRP was applied. On half of the span, three strips of CFRP fabric (each approximately 610 mm wide) were fully wrapped around the specimen, while a steel beam-and-bar assembly further enhanced the shear strength of the haunched half of the span. Loading resumed, and at 1911 kN, a region near the loading point was strengthened with a high-strength mortar surrounded by a steel enclosure. Thereafter, loading recommenced and reached 2528 kN. At this stage, the carbon fabric failed by ripping at the top edge near the load application point, and a substantial amount of concrete suddenly spalled off. The premature shear failure observed in the control beam was changed to a ductile flexural failure in the CFRP-repaired beam.

The asymmetrical geometrical and loading conditions of the De Rose beam specimen made it necessary to model the entire beam in the finite element analysis. As was done for the De Rose slab, the beam analysis was divided into two parts to model the repair sequence. The predicted response of the CFRP-repaired beam is compared to the test data in Fig. 9(c). In the analysis including bond-slip using the elastic-plastic bond law (FE-EP), the repaired beam failed in a shear-flexural mode at a load of 2465 kN—2% lower than the actual result. A previous analysis by Bucci, in which perfect bond conditions were assumed (FE-P), resulted in a higher postyielding stiffness, and greatly underestimated the

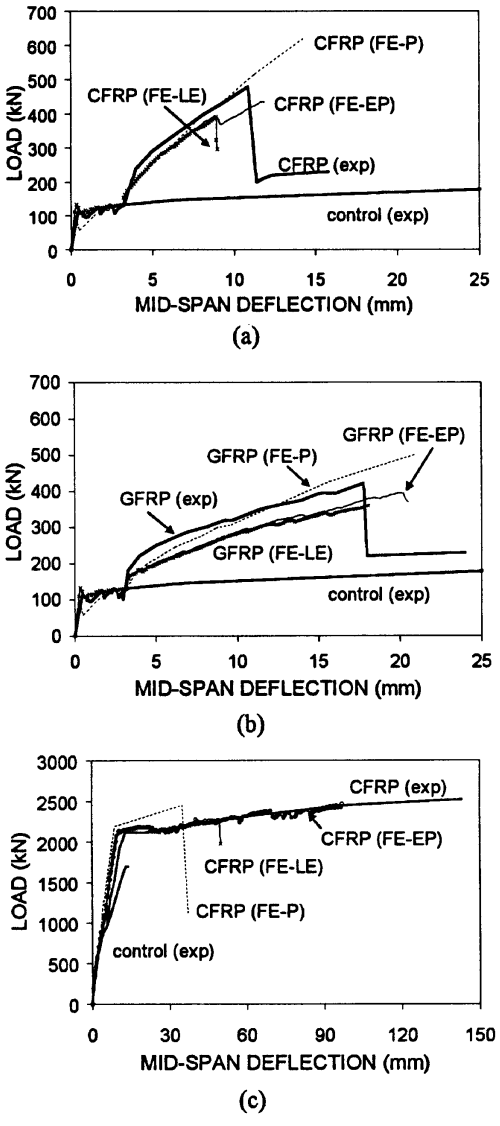

Fig. 9—Load-deflection curves for De Rose specimens: (a) CFRP-repaired slab; (b) GFRP-repaired slab; and (c) beams.

deflection at failure. The linear elastic bond model (FE-LE) also predicted an early failure of the beam.

RWOA specimens

The final set of specimens analyzed was the three RWOA beams described previously as part of the experimental program. For each beam, half of the specimen was modeled, with each CFRP strip represented by five columns of truss elements. In several concrete elements near the loading point, out-of-plane reinforcement was added to simulate the confinement effects provided by the loading plate.

The predicted load-deflection curves, along with the comparisons against the experimental results, are plotted in Fig. 10. For all three specimens analyzed using the FE-EP assumption, the postcracking stiffnesses matched reasonably well with the test data. The yield loads, post-yielding stiffnesses, and deflections at failure, however, were overestimated in the analyses. These discrepancies may be attributed to the limitation of using a two-dimensional program that cannot capture the outwards splitting of the side concrete covers and the downward shearing of the beam's central section. In addition, the modeling

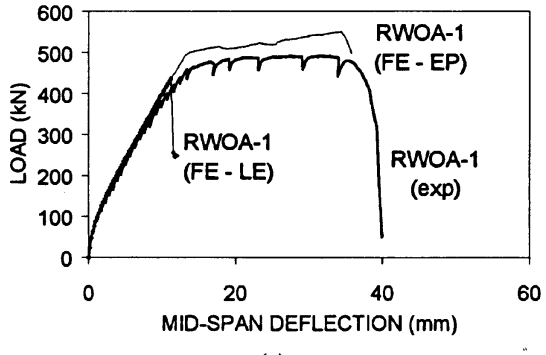

(a)

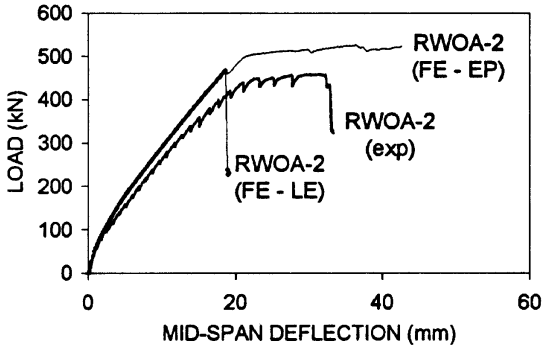

(b)

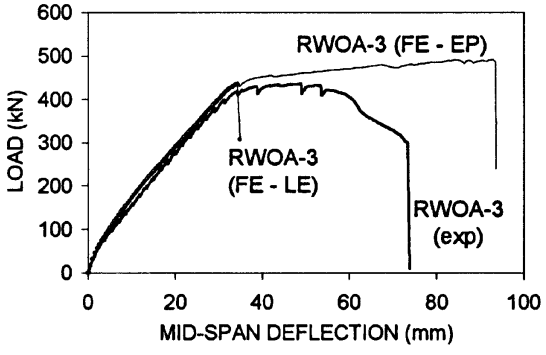

(c)

Fig. 10—Load-deflection curves for RWOA specimens: (a) RWOA-1; (b) RWOA-2; and (c) RWOA-3.

of the out-of-plane reinforcement near the loading point may have contributed to the excess ductility. When the linear elastic bond law (FE-LE) was applied, premature shear failures were found to occur prior to the yielding of the flexural reinforcement. On the other hand, perfect bond assumptions produced similar results as the elastic-plastic bond relationship because the failure of the members was governed by shear-flexural behavior.

DISCUSSION OF ANALYTICAL RESULTS

The incorporation of bond elements into the finite element (FE) program enabled better predictions of the response of members strengthened in flexure or shear with FRP composites, both in terms of member stiffness and capacity. The accuracy of these estimations, however, depended on the bond stress-slip relationship that was chosen for the analyses. It was found that the linear elastic bond law was appropriate only when the failure was dominated by sudden delamination of the FRP plate, which is expected to occur when the shear strength of the epoxy is low. On the other hand, in the specimens utilizing stronger epoxies, the failure was predominantly through the peeling of the concrete cover, which was critical due to its lower shear strength (represented by the concrete's modulus of rupture). For these specimens, the analyses were more accurate when the elastic-plastic bond relationship was applied.

After performing FE analyses of several sets of specimens, it can be suggested that the cutoff on the maximum bond stress is a function of the concrete's modulus of rupture, the maximum slip is a function of the shear modulus of the epoxy, and the existence of the plastic range in the bond law depends on the shear strength of the epoxy. As for the ultimate slip that can be sustained, more work is needed to estimate its value. Because many interrelated factors influence the bond stress-slip relationship, further studies are required. Despite some minor uncertainties regarding the bond constitutive relationship, the nonlinear finite element analyses can give fairly accurate predictions of the overall behavior of RC members strengthened with externally bonded FRP composites.

For future work involving finite element analysis, a two-dimensional contact element should be implemented. This type of element would permit slippage in both x- and y-directions simultaneously and would provide for continuous bond stress distribution between the concrete and FRP. In addition, alternative formulations of the bond law that have been recently proposed by various researchers should be examined.

CONCLUSIONS

The results from an experimental program have shown that externally bonded FRP composites can enhance the strength and stiffness of RC members and can change the failure mode of shear-critical beams. Premature debonding of the FRP laminates, however, must be prevented to avoid reductions in ductility and to fully use the capacity of the strengthening material.

Based on the currently available shear stress-slip relationships, bond elements have been successfully incorporated into a nonlinear finite element program. Studies undertaken have shown that accounting for bond slip between concrete and FRP is viable, and that it is necessary to model the interface behavior if an accurate prediction of the response of FRP-strengthened RC members is to be made. Nonetheless, a more clearly defined constitutive relationship must be developed for the bond elements to further improve modeling capability. To perform corroboration with test specimens, experimental data regarding strengthening with FRP composites should be reported in detail in the published literature, including member geometry, mechanical properties of the materials used, and the test procedures, along with the test observations and results.

ACKNOWLEDGMENTS

The funding for this research was provided by the National Science and Engineering Research Council (NSERC), and the repair materials for the experimental program were contributed by R. J. Watson Inc. and Fyfe Co.

REFERENCES

1. Arduini, M., and Nanni, A., "Behavior of Precracked RC Beams Strengthened with Carbon FRP Sheets," *Journal of Composites for Construction*, V. 1, No. 2, 1997, pp. 63-70.

2. Ross, C. A.; Jerome, D. M.; Tedesco, J. W.; and Hughes, M. L., "Strengthening of Reinforced Concrete Beams with Externally Bonded Composite Laminates," *ACI Structural Journal*, V. 96, No. 2, Mar.-Apr. 1999, pp. 212-220.

3. Vecchio, F. J., and Bucci, F., "Analysis of Repaired Reinforced Concrete Structures," *Journal of Structural Engineering*, V. 125, No. 6, 1999, pp. 644-652.

4. Bresler, B., and Scordelis, A. C., "Shear Strength of Reinforced Concrete Beams," ACI JOURNAL, *Proceedings* V. 60, No. 1, Jan. 1963, pp. 51-72.

5. ASTM, "Standard Test Method for Tensile Properties of Polymer Matrix Composite Materials (ASTM D 3039/D 3039M)," West Conshohocken, Pa., 2000.

6. Wong, R. S. Y., "Towards Modeling of Reinforced Concrete Members with Externally Bonded Fibre Reinforced Polymer (FRP) Composites," MASc thesis, University of Toronto, Toronto, Canada, 2001, 298 pp.

7. Vecchio, F. J., and Collins, M. P., "The Modified Compression Field Theory for Reinforced Concrete Elements Subjected to Shear," ACI JOURNAL, *Proceedings* V. 83, No. 2, Mar.-Apr. 1986, pp. 219-231.

8. Vecchio, F. J., "Nonlinear Finite Element Analysis of Reinforced Concrete Membranes," *ACI Structural Journal*, V. 86, No. 1, Jan.-Feb. 1989, pp. 26-35.

9. Vecchio, F. J., "Reinforced Concrete Membrane Element Formulations," *Journal of Structural Engineering*, V. 116, No. 3, 1990, pp. 730-750.

10. Aprile, A.; Spacone, E.; and Limkatanyu, S., "Role of Bond in RC Beams Strengthened with Steel and FRP Plates," *Journal of Structural Engineering*, V. 127, No. 12, 2001, pp. 1445-1452.

11. Homam, S. M.; Sheikh, S. A.; Pernica, G.; and Mukherjee, P. K., "Durability of Fibre Reinforced Polymers (FRP) Used in Concrete Structures," *Research Report*, Department of Civil Engineering, University of Toronto, Toronto, Canada, 2000, 202 pp.

12. Sato, Y., "Shear Strengthening of Reinforced Concrete Beam Using Continuous Fibre Sheet," PhD dissertation, Kyoto University, Japan, 2000, 213 pp.

13. Ngo, D., and Scordelis, A. C., "Finite Element Analysis of Reinforced Concrete Beams," ACI JOURNAL, *Proceedings* V. 64, No. 3, Mar. 1967, pp. 152-163.

14. Keuser, M., and Mehlhorn, G., "Finite Element Models for Bond Problems," *Journal of Structural Engineering*, V. 113, No. 10, 1987, pp. 2160-2173.

15. Žarnić, R.; Gostić, S.; Bosiljkov, V.; and Bokan-Bosiljkov, V., "Improvement of Bending Load-Bearing Capacity by Externally Bonded Plates," *Specialist Techniques and Materials for Concrete Construction*, Proceedings of the International Conference on Creating with Concrete, Dundee, Scotland, 1999, pp. 433-442.

16. El-Refaie, S. A.; Ashour, A. F.; and Garrity, S. W., "Strengthening of Reinforced Concrete Continuous Beams with CFRP Composites," *Proceedings of the International Conference on Structural Engineering, Mechanics and Computation*, V. 2, Elsevier Science Ltd., Oxford, UK, 2001, pp. 1591-1598.

17. De Rose, D., and Sheikh, S. A., "Rehabilitation of a Concrete Structure Using Fibre Reinforced Plastics," *Research Report*, Department of Civil Engineering, University of Toronto, Toronto, Ontario, Canada, 1997, 170 pp.